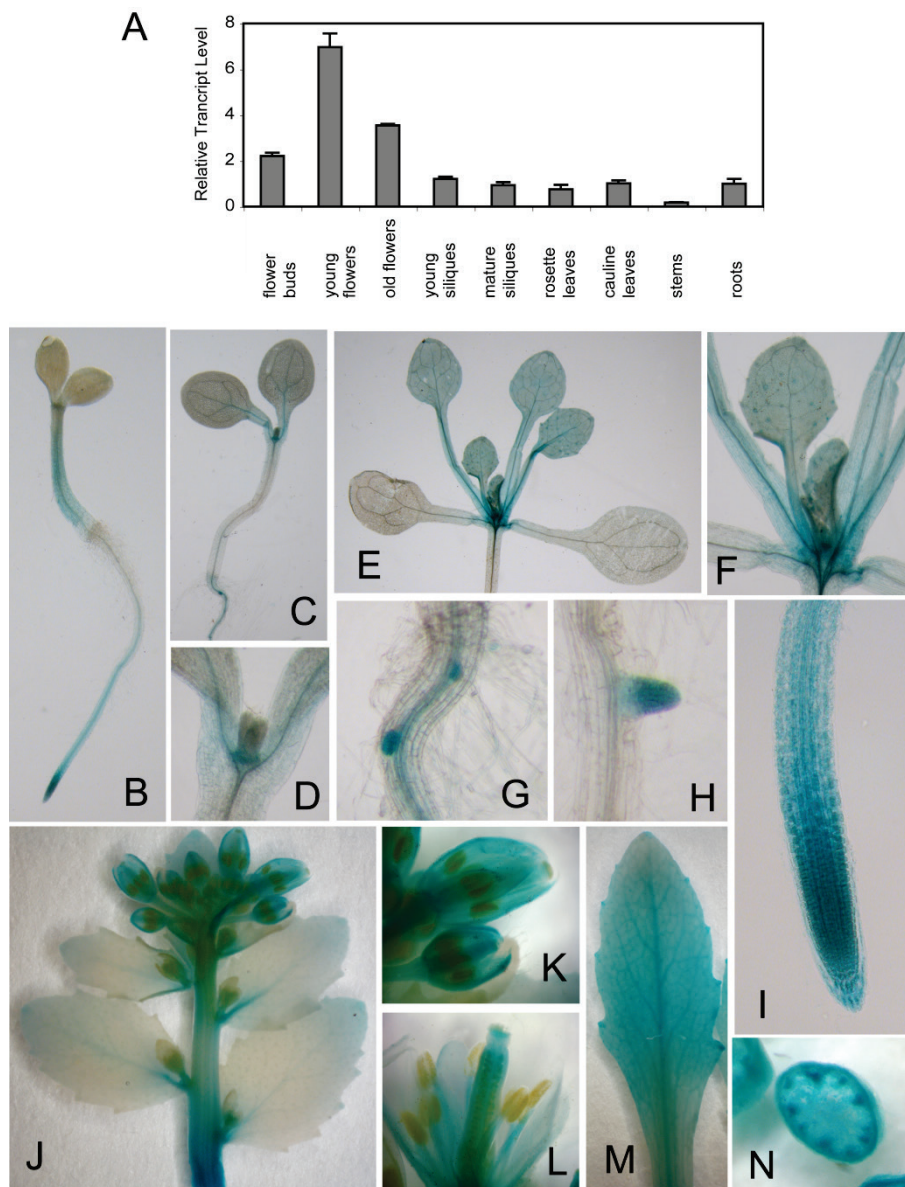


Supplemental Figure 1. Positions of T-DNA Insertion in *CRK5* and qRT-PCR Analysis of Transcription of *crk5* Mutant Alleles.

(A) Schematic map positions of T-DNA insertions in the *crk5-1* (MPIZ38225) and *crk5-2* (SALK_003774) alleles are indicated by triangles above the map. Dark grey boxes label 5' and 3' UTRs, light grey boxes are exons, and lines represent introns. Positions of oligonucleotide primers used in quantitative real-time PCR (qRT-PCR) analysis are indicated by arrows. (B) qRT-PCR measurement of *CRK5* transcript levels in wild type and the *crk5-1* and *crk5-2* insertion mutants. All qRT-PCR measurements were performed in triplicates. Bars label standard error (SE) of measurements performed with three biological replicates. (C) Schematic map of *CRK5-GFP* and *CRK5-GUS* gene fusions used for genetic complementation of *crk5-1* mutation and cellular localization studies.



Supplemental Figure 2. qRT-PCR Measurement of *CRK5* Transcript Levels and Detection of *CRK5*-GUS Expression in Different Organs.

(A) qRT-PCR measurement of *CRK5* transcript levels in different organs of wild-type *Arabidopsis* plants. Relative transcript levels were standardized to *GAPDH-2* (At1g13440, Czechowski et al. 2005). The qRT-PCR measurements were performed in triplicates. Bars label standard error (SE) of measurements performed with three biological replicates. (B-N) Histochemical detection of *CRK5*-GUS expression in hypocotyls, roots, root apices, apical meristems and cotyledons of 7 (B-D) and 14 (E-F) days old light grown seedlings. *CRK5*-GUS shows high level of expression in the root stele and lateral root primordia (G-H), as well as in the root apex (I). In the inflorescence, *CRK5*-GUS is expressed in the vasculatures of cauline leaves, sepals, petals, anther filaments and pistils of flowers (J-M). In stem cross sections, *CRK5*-GUS activity is localized in the vascular bundles (N).

```

*      20      *      40      *
AtCRK1 : MGICHGKP-----VEQQSKSLPVSGETNEA-----PTNSQPPAKSS- : 36
AtCRK2 : MGGCTSKPS--SSVKPNPYAPKDAVLQNDSTPAH----PGKSPVRSSPA- : 44
AtCRK3 : MGQCYGKVN--QSKQN-GEEEANTT-----TYV--VSGDGNQIQP--- : 35
AtCRK4 : MGHCYSRNI--SA----VEDD-ELPT-----GNGE--VSNQPSQNHRRH-- : 34
AtCRK5 : MGLCTSKPN-----SSNSDQTPARNSPLPASESVKPSSSSVNGEDQ- : 41
AtCRK6 : MGHCYSRNI--ST----VDDDELPS-----ATAQ--LPHRSHQNHQT- : 36
AtCRK7 : MGLCHGKP-----IEQQSKNLPISNEIEET-----PKNSSQKAKSS- : 36
AtCRK8 : MGGCTSKPSTSSGRPNPFAPGNDYPQIDDFAPDH----PGKSPIPTPSA- : 45
LeCRK1 : MGQCCSK-----GVSGENGGSVVA--IGDGNSA--VSTNNRPKPPP-- : 37
NtCBK1 : MGHCCSK-----GVTADNDGHVVS--VVDGNS--VSTNNRPKPSP-- : 37
NtCBK2 : MGACTSKPS-----NFSVDDITVAGDGAIFP-----VKSGSPSNDDDV- : 37
DcCRK1 : MGICVSKPS-P--EPDLHNHHTSLPVNDTSLP-----PQDNSIPPKDI- : 40
ZmMCK1 : MGQCYGKAR--GASSR-ADHDADPSGAGSVAPPSP--LPANGAPLP--- : 41
ZmMCK2 : MGQCYGKAG--GASSRRADHD-----DAVAPPSP--LPANGAPTPPQQ : 40
OsCBK1 : MGLCHGKSA-AVLEPTVEEEEEGATRVAEAAAA-----PAKPASPASA- : 43
    
```

N-terminal myristoylation/
palmitoylation motive

```

60      *      80      *      100
AtCRK1 : ---G-----FFFVSPSP---VP-SLFKSSSSV---S : 57
AtCRK2 : ---V-----KASPFFFFFYTPSPARHRRN---KSRD-GG---G : 71
AtCRK3 : LTPVNYGRANTPARSSNPSP---WPSP---FPHSASPLSGVSPS : 76
AtCRK4 : ---ASIPQSPVASGTPEV--NSTNISP---FQ---SLPAGV--A : 66
AtCRK5 : ---CVTTTNNE---GKKSPFFFFFYSPSPAHYFFS---KKTPA--R : 75
AtCRK6 : ---SSSSSIPQSPATS---EV--NPNISP---FQ---SLPAGV--A : 68
AtCRK7 : ---G-----FFFVSPSP---LP-SLFKTSPAV---S : 57
AtCRK8 : ---A-----KASPFFFFFYTPSPARHRRN---KSRDVGG---G : 73
LeCRK1 : -SPVR-QSVGNGMSYTNNSTP-AHSETTASP---FQ---SPYPAGIAPS : 76
NtCBK1 : -SPARPQSVGNGTSYTNNSTP-AHSETTASP---FQ---SPYPAGIPPS : 77
NtCBK2 : ---NSHQTRNDEPSVGKKSPFFFFFYSPSPAHYLFS---KKSPAT---N : 76
DcCRK1 : ---AIPAQDNNKPP-GKKSPFLPFFYSPSPAHFLFS---KKSPAV---G : 78
ZmMCK1 : ATPRRHKSGSTTPVHHHQAATPGAAAWPSP---YPAGASPLPAGVSPS : 87
ZmMCK2 : ATPGRRKSGSATPVHHHQAAT---AWPSP---YPAGASPLPAGVSPS : 82
OsCBK1 : ---AAAAAKPGTPK---QHKFFFYLPSP---LPASSYKGSPA----- : 76
    
```

```

*      120      *      140      *
AtCRK1 : S---S-VSSTELRI-FKRFFFPPSPAKHIRAFLARRYCS--VKPNEVSIP : 100
AtCRK2 : GE-SKSVTSTELRQ-LARAFFPPSPARHIRDVLRRRK-----EKKEAALP : 114
AtCRK3 : P---ARTSTERRF-FRRFFFPPSPAKHIKASLKRLGV---KPKEGPIP : 118
AtCRK4 : P---SPARTEGRK-FKWFFFPPSPAKPIMAALRRRRRCA-PPQPRDEPIP : 110
AtCRK5 : SPATNSTEKRF-FKRFFFPPSPAKHIRAVLARRHGS--VKPNESAIP : 122
AtCRK6 : P---SPARTEGRK-FKWFFFPPSPAKPIMAALRRRRRCT-APHPRDGPIP : 112
AtCRK7 : S---SVSSTELRI-FKRFFFPPSPAKHIRALLARRHGS--VKPNEASIP : 101
AtCRK8 : GE-SKSLTSTELRQ-LRRAFFPPSPAKHIRAALRRRK-----GKKEAALS : 116
LeCRK1 : P---SPVGTERRK-FKWFFFPPSPAKPILSAILKROCGTSVKPKEGPIP : 121
NtCBK1 : P---SPVGTERRK-FKWFFFPPSPAKPILSAILKROCGTSAKPKEGPIP : 122
NtCBK2 : A---SSNSTEMRF-FKRFFFPPSPAKHIRSLLARRHCT--VKPNESAIP : 119
DcCRK1 : SPAAGSNSTEKRL-F---PFFFPPSPAKHIKAAWARRHCS--VKPNEAAIP : 123
ZmMCK1 : P---AR-STERRF-FKRFFFPPSPAKHIKATLAKRLCG--GKPKEGTIP : 129
ZmMCK2 : P---AR-STERRF-FKRFFFPPSPAKHIKATLAKRLCG--GKPKEGTIP : 124
OsCBK1 : N---SSVASTEARGGFKRFFFFPPSPAKHIRALLARRHGS--VKPNEASIP : 121
    
```

Predicted NLS

```

160      *      180      *      200
AtCRK1 : EGKECE-----I--G-----LDKSFGFSK : 117
AtCRK2 : AARQQKEE---EEREEV--G-----LDKRFGFSK : 138
AtCRK3 : EER-----GT-----EPEQSLDKSFGYGK : 137
AtCRK4 : EDS-----EDVVDHG-GDSGG-----GER-LDKNFGFGK : 137
AtCRK5 : EGSEAE-----GGGV--G-----LDKSFGFSK : 142
AtCRK6 : EDS-----EA-----G-GSGGGI-----GER-LDKNFGFAK : 136
AtCRK7 : EGSECE-----V--G-----LDKKFGFSK : 118
AtCRK8 : GVTQLTTEVPQREEEEEV--G-----LDKRFGFSK : 144
LeCRK1 : EDE-----GG-----EGERQLDKSFGYPK : 140
NtCBK1 : EDE-----GG-----EGERQLDKSFGYPK : 141
NtCBK2 : EGNESEVG---DGGGA--G-----LDKSFGFSK : 142
DcCRK1 : ENNEVD-----GGA--G-----LDKSFGFSK : 142
ZmMCK1 : EEG-----GAGAGAGAGAGAAVGADSAEADRPLDKIFGFAK : 168
ZmMCK2 : EEG-----GAGV-----AADSAEAERPLDKIFGFAN : 150
OsCBK1 : ESGEPG-----V--A-----LDKGFGFSR : 138
    
```

```

                *           220           *           240           *
AtCRK1 : QFASHYEIDGFEVGRGHFGYTCSAKCKKGSLLKQEVAVKVIIPKSKMTAIA : 167
AtCRK2 : ELQSRTELEDFEIGRGHFGYTCSAKCKKGSLLKQEVAVKVIIPKSKMTSAIS : 188
AtCRK3 : NFGAKYELCKREVGRGHFGHTCSGRCKKGDILKDHPIAVKIIISKAKMTAIA : 187
AtCRK4 : NFEGKYELCKREVGRGHFGHTCWAKAKKGMKRNQTVAVKIIISKAKMTSTLS : 187
AtCRK5 : SFASKYELCKREVGRGHFGYTCAAKCKKGDNRQQVAVKVIIPKAKMTAIA : 192
AtCRK6 : NFEGKYELCKREVGRGHFGHTCWAKAKKGMKRNQTVAVKIIISKAKMTSALS : 186
AtCRK7 : QFASHYEIDGFEVGRGHFGYTCSAKCKKGSLLKQEVAVKVIIPKSKMTAIA : 168
AtCRK8 : EFHSEVLEDFEIGRGHFGYTCSAKCKKGSLLKQEVAVKVIIPKSKMTAIA : 194
LeCRK1 : NLTSKYELCKREVGRGHFGHTCWAKCKKGSLLKQEVAVKVIIPKAKMTAIA : 190
NtCBK1 : NLTAKELEDFEIGRGHFGHTCWAKCKKGSLLKQEVAVKVIIPKAKMTAIA : 191
NtCBK2 : NFVNKYEMGEFEVGRGHFGYTCRAKCKKGEFKQEVAVKVIIPKAKMTAIA : 192
DcCRK1 : KFGSKFEVDFEFEVGRGHFGYTCRAKCKKGEFKQEVAVKVIIPKAKMTAIA : 192
ZmCRK1 : NFGAKYDLCKREVGRGHFGHTCSAVVKKGEHRGHTAVKIIISKAKMTAIA : 218
ZmMCK2 : NFGAKYDLCKREVGRGHFGHTCSALVKKGEYKGHAVAVKIIISKAKMTAIA : 200
OsCBK1 : HFAAKYELCKREVGRGHFGYTCAAKCKKGSLLKQEVAVKVIIPKAKMTAIA : 188
    
```

Serine/threonine protein kinase catalytic domain

ATP-binding motive

```

                260           *           280           *           300
AtCRK1 : IEDVRSREVKMLRALIIGHKNLWQFYDAFEDDENVYIIMELCKGGELLDKIL : 217
AtCRK2 : IEDVREVKILRALSGHQNLWQFYDAFEDNANVYIIMELCKGGELLDRIIL : 238
AtCRK3 : IEDVREVKLLKSLSGHKYLIKYYDACEANVYIIMELCKGGELLDRIIL : 237
AtCRK4 : IEDVREVKLLKSLSGHRHMWKFYDVEDADNVFVIMELCKGGELLDRIIL : 237
AtCRK5 : IEDVREVKILRALSGHNNLPHFYDAYEDHDNVYIIMELCKGGELLDRIIL : 242
AtCRK6 : IEDVREVKLLKSLSGHSHMWKFYDVEDSDNVFVIMELCKGGELLDRIIL : 236
AtCRK7 : IEDVREVKILRALIIGHKNLWQFYDAFEDDENVYIIMELCKGGELLDKIL : 218
AtCRK8 : IEDVREVKILRALIIGHKNLWQFYDAFEDNANVYIIMELCKGGELLDRIIL : 244
LeCRK1 : IEDVREVKILKALSGHQNLWQFYDAFEDANVYIIMELCKGGELLDRIIL : 240
NtCBK1 : IEDVREVKILKALSGHQNLWQFYDAFEDANVYIIMELCKGGVLLDRIIL : 241
NtCBK2 : IEDVREVKILRALIIGHNNLWQFYDAYEDPNVYIIMELCKGGELLDRIIL : 242
DcCRK1 : IEDVREVKILRALIIGHNNLWQFYDAFEDHTNVYIIMELCKGGELLDRIIL : 242
ZmMCK1 : IEDVREVKILKALSGHDNLWRFYDACEANVYIIMELCKGGELLDRIIL : 268
ZmMCK2 : IEDVREVRILKALSGHNNLWQFYDACEANVYIIMELCKGGELLDRIIL : 250
OsCBK1 : IEDVREVRILSSLAGHSNLWQFYDAYEDEENVYIIMELCKGGELLDRIIL : 238
    
```

Serine/threonine protein kinase catalytic domain

Active site

```

                *           320           *           340           *
AtCRK1 : QRGKYSEDDAKKVMQIILSVVAYOHLQGVVHRDLKPENFLFSTKDETSF : 267
AtCRK2 : ARGKYSEDDAKAVLQIILNVVAFQHLQGVVHRDLKPENFLYTSKEDNSM : 288
AtCRK3 : ARGKYPEDDAKAVIQQIILTVVSFOHLQGVVHRDLKPENFLFTSSREDS : 287
AtCRK4 : ARGGRYPEVDAKRILMQIILSATAFQHLQGVVHRDLKPENFLFTSKEDAI : 287
AtCRK5 : SRGGKYTEEDAKTVMQIILNVVAFQHLQGVVHRDLKPENFLFTSKEDTS : 292
AtCRK6 : ARGGRYPEVDAKRILMQIILSATAFQHLQGVVHRDLKPENFLFTSKEDAV : 286
AtCRK7 : QRGKYSEVDAKVMQIILSVVAYOHLQGVVHRDLKPENFLFTTKDESSP : 268
AtCRK8 : ARGKYSEDDAKPVIQIILNVVAFQHLQGVVHRDLKPENFLYTSKEDNSQ : 294
LeCRK1 : SRGGRYTEEDAKSIVQIILNVVAFQHLQGVVHRDLKPENFLFAKDEDS : 290
NtCBK1 : SRGGRYTEEDAKSILVQIILNVVAFQHLQGVVHRDLKPENFLFTSKEDAP : 291
NtCBK2 : SRGGKYTEEDAKSVMQIILKVVAFQHLQGVVHRDLKPENFLFTSKEDNAQ : 292
DcCRK1 : SRGGKYTEEDAKAVMQIILNVVAFQHLQGVVHRDLKPENFLFKSKEDSD : 292
ZmMCK1 : ARGGRYTEEDAKAVIQQIILSVVAFQHLQGVVHRDLKPENFLFTTRDESAP : 318
ZmMCK2 : ARGGRYTEEDAKAVIQQIILSVVAFQHLQGVVHRDLKPENFLFATRDESAP : 300
OsCBK1 : ARGKYSEVDAKVMQIILSVVAFQHLQGVVHRDLKPENFLFSSKEDNSA : 288
    
```

Serine/threonine protein kinase catalytic domain

ATP-binding motive

```

                360           *           380           *           400
AtCRK1 : LKALDFGLSDYVREKDERLNDIVGSAYYVAPEVLHRTYGTEDMWSIGVIA : 317
AtCRK2 : LKVIDFGLSDFVREKDERLNDIVGSAYYVAPEVLHRSYSTEADVWSIGVIA : 338
AtCRK3 : LKALDFGLSDFVREKDERLNDIVGSAYYVAPEVLHRSYSLEADIWSIGVIT : 337
AtCRK4 : LKVIDFGLSDFVRYDQRLNDVVGSAAYYVAPEVLHRSYSSTEADMWSIGVIS : 337
AtCRK5 : LKALDFGLSDYVREKDERLNDIVGSAYYVAPEVLHRSYSSTEADIWSVGIV : 342
AtCRK6 : LKVIDFGLSDYVREKDERLNDVVGSAAYYVAPEVLHRSYSSTEADIWSIGVIS : 336
AtCRK7 : LKALDFGLSDYVREKDERLNDIVGSAYYVAPEVLHRTYGTEDMWSIGVIA : 318
AtCRK8 : LKALDFGLSDFVREKDERLNDIVGSAYYVAPEVLHRSYSTEADVWSIGVIA : 344
LeCRK1 : MKVIDFGLSDFVREKDERLNDIVGSAYYVAPEVLHRSYSSTEADMWSIGVIT : 340
NtCBK1 : MKVIDFGLSDFVREKDERLNDIVGSAYYVAPEVLHRSYSSTEADMWSIGVIT : 341
NtCBK2 : LKALDFGLSDFVREKDERLNDIVGSAYYVAPEVLHRSYSSTEADVWSIGVIA : 342
DcCRK1 : LKALDFGLSDYVREKDERLNDIVGSAYYVAPEVLHRSYSSTEADVWSIGVIS : 342
ZmMCK1 : MKLIDFGLSDFVREKDERLNDIVGSAYYVAPEVLHRSYSMEADIWSIGVIT : 368
ZmMCK2 : MKLIDFGLSDFVREKDERLNDIVGSAYYVAPEVLHRSYSMEADIWSIGVIT : 350
OsCBK1 : MKVIDFGLSDFVREKDERLNDIVGSAYYVAPEVLHRSYGTEDMWSIGVIV : 338
    
```

Serine/threonine protein kinase catalytic domain

T-loop

```

*           420           *           440           *
AtCRK1 : YILLGSRPFWARTESGIFRAVLKAEPNFEEAPWPSISPEAVDFVKRLLN : 367
AtCRK2 : YILLGSRPFWARTESGIFRAVLKADPSFDEFPWPSISFEAKDFVKRLLY : 388
AtCRK3 : YILLGSRPFWARTESGIFRIVLRTEPNYDDVPWPCSSEKDFVKRLLN : 387
AtCRK4 : YILLGSRPFYGRTESAIFRCVLRANPNFEDMPWPSISPTAKDFVKRLLN : 387
AtCRK5 : YILLGSRPFWARTESGIFRAVLKADPSFDDFPWPTLSSEARDFKVRLLN : 392
AtCRK6 : YILLGSRPFYGRTESAIFRCVLRANPNFEDLPWPSISPIAKDFVKRLLN : 386
AtCRK7 : YILLGSRPFWARSESIGIFRAVLKAEPNFEEAPWPSISPEAVDFVKRLLN : 368
AtCRK8 : YILLGSRPFWARTESGIFRAVLKADPSFDEFPWPTLSSDAKDFVKRLLF : 394
LeCRK1 : YILLGSRPFWARTESGIFRSVLRADPNFEDSPWPAVSAEARDFKVRLLN : 390
NtCBK1 : YILLGSRPFWARTESGIFRSVLRADPNFEDSPWPSVSAEARDFKVRLLN : 391
NtCBK2 : YILLGSRPFWARTESGIFRAVLKADPSFDEQPWPTLSSSEAKDFVKRLLN : 392
DcCRK1 : YILLGSRPFWARTESGIFRAVLKANLSFDEFPWPSVSSSEAKDFVKRLLN : 392
ZmMCK1 : YILLGSRPFWARTESGIFRSVLRADPNFDDSPWPSVSAEAKDFVKRFLN : 418
ZmMCK2 : YILLGSRPFWARTESGIFRFVLRADPNFDDSPWPSVSAEAKDFVKRFVN : 400
OsCBK1 : YILLGSRPFWARTESGIFRAVLKADPSFEEAPWPTLSAEAKDFVRRLLN : 388
    
```

Serine/threonine protein kinase catalytic domain

```

460           *           480           *           500
AtCRK1 : KDYRKRRLTAAQALCHFWLVGSHE-LKIPSDMIYKLVKVIYIMSTSLRKSA : 416
AtCRK2 : KDPRKRMTASQALMHPWIAGYKK-IDIPFDLIIFKQIKAYLRSSSLRKAA : 437
AtCRK3 : KDYRKRMTAVQALTHEFWLRDSDSR--VPLDILIIYKLVKAYLHATPLRRAA : 435
AtCRK4 : KDHRKRMTAAQALAHFWLRDENP--GILLDFSVYKLVKSYLRASPRRAA : 435
AtCRK5 : KDPRKRMTAAQALSHPWIKDSND-AKVPMDLIVFKLMRAYLRSSSLRKAA : 441
AtCRK6 : KDHRKRMTAAQALAHFWLRDENP--GILLDFSIYKLVKSYLRASPRRAA : 434
AtCRK7 : KDYRKRRLTAAQALCHFWLVGSHE-LKIPSDMIYKLVKVIYIMSSSLRKSA : 417
AtCRK8 : KDPRKRMTASQALMHPWIRAYNTDMNIPFDLIIFKQIKAYLRSSSLRKAA : 444
LeCRK1 : KDHRKRMTASQALTHEFWLRDENP--FVPLDILIIFKLVKSYLRTPSLKRAA : 438
NtCBK1 : KDHRKRMTASQALAHFWLRDENP--VPLDILIIFKLVKSYLRASPLKRAA : 439
NtCBK2 : KDPRKRMTAAQALCHFWIKNSHN-MEEPDLIIIFKLMKAYLRSSSLRKAA : 441
DcCRK1 : KDPRKRMTAAQALCHSWIKNSND-IKFPLDILIVFKLMKVIYIMSSSLRKAA : 441
ZmMCK1 : KDYRKRMTAVQALTHEFWLRDEQR--QIPLDILIIFRIVKQYLRATPLKRLA : 466
ZmMCK2 : KDYRKRMTAVQALTHEFWLRDEQR--QIQLDLIVFRIVKQYLRATPLKRLA : 448
OsCBK1 : KDYRKRMTAAQALCHFWIRGTEE-VKLPDMLIYRILMAYLRSSSLRRAA : 437
    
```

Serine/threonine protein kinase catalytic domain

Autoinhibitory domain

Calmodulin-binding motif

```

*           520           *           540           *
AtCRK1 : LAALAKTLITVPOIAYLREQFTLLGFSKNGYISMQNYKTATLKSSTDAMKD : 466
AtCRK2 : LMALSKTLITDDEILYLKAQFAHLAPNKNGLITLDSIRLALATNATEAMKE : 487
AtCRK3 : LKALAKALITENELIYLRQAQFMLLGNKDGVSYLENFKTALMQNATDAMRE : 485
AtCRK4 : LKALSKAIPDEELVFLKAQFMLLDP--KDGGLSLNCFMTALTRYATDAMME : 484
AtCRK5 : LRALSKTLITVDELFYLREQFALLEPSKNGTISLENIKSALMKMATDAMKD : 491
AtCRK6 : LKSLSKAIPPEELVFLKAQFMLEP--EDGGLHLHNFETALTRYATDAMIE : 483
AtCRK7 : LAALAKTLITVPOIAYLREQFTLLGFSKNGYISMQNYKTATLKSSTBATKD : 467
AtCRK8 : LRALSKTLIKDEILYLKTFSLAPNKDGLITMDTIRMALASNATEAMKE : 494
LeCRK1 : LKALSKALTEEELIYLKAQFNLEP--KAGFVSLDNFRMALMKTQTTDAMRE : 487
NtCBK1 : LKALSKALTEEELIYLRAQFNLEP--KDGRLVSLNFKMALTKQMTDAMRE : 488
NtCBK2 : LRALSKTLITVDELFYLKEQFVLEPTKNGTISLENIKQALMKNSTDAMKD : 491
DcCRK1 : LRALSKTLITVDELFYLKEQFVLEPTKNGTISLENIKQALMKNSTDAMKD : 491
ZmMCK1 : LKALSKALSEDEILYLRLQFKLEP--RDGIVSLDNFRTALTRYVTDAMRE : 515
ZmMCK2 : LKALSKALREDEILYLRLQFKLEP--RDGIVSLDNFRTALTRYVTDAMRE : 497
OsCBK1 : LRALAKTLITDQIYLYLREQFELIGENKSDLITLQNLKALMKNSTNAMKD : 487
    
```

Degenerated EF hand

```

560           *           580           *           600
AtCRK1 : SRVDFVHMTSCLQYKKLDFEEFCASLSVYOLEAMETWEQHARRAYELF : 516
AtCRK2 : SRIPDFLALNGLQYKGMDFEEFCASISVHGHESLDCWEQIRHAYELF : 537
AtCRK3 : SRVPEILHMTESLARKMYFEEFCAAISIHOLEAVDAWEQIATAGFOHF : 535
AtCRK4 : SRLPDLINMQPLAQKKLDFEEFCAAAVSVYOLEALEWEQIATSAFEHF : 534
AtCRK5 : SRIFEFLGQISALQYRRMDFFEEFCAAALSVOLEALDRWEQHARCAAYELF : 541
AtCRK6 : SRLPDLINMQPLAHKKLDFEEFCAAAVSVYOLEALEWEQIATVAFEHF : 533
AtCRK7 : SRVLDVHMTSCLQYKKLDFEEFCASLSVYOLEAMETWEQHARRAYELY : 517
AtCRK8 : SRIFEFLALNGLQYRGMDFEEFCAAAINVHGHESLDCWEQIRHAYELF : 544
LeCRK1 : ARVLDIINLEPPLSVKQMDFFEEFCAAAIISTYOLEALENWEHIASAENYF : 537
NtCBK1 : SRVFDLNLNMEPLSVKPLDFEEFCAAAIISTYOLEALENWEQIASAFEHF : 538
NtCBK2 : ARMHDELASLNALQYRRMDFFEEFCAAALSVOLEALDRWEQHARCAAYEIF : 541
DcCRK1 : SRVLDLVSINLALQYRRMDFFEEFCAAALSVOLEALDRWEQHARCAAYDFL : 541
ZmMCK1 : SRVLEFQHALEPLAVRKMDFFEEFCAAAIISPYOLEALERWEIAGTAFQHF : 565
ZmMCK2 : SRVLEFLHADPLAVRKMDLEEFCAAISPYOLEALESWEEIAGTAFQHF : 547
OsCBK1 : SRVDFVNTISNIQYRKLDFEEFSAAIISVYQMEGLTWEQHARQAYEFF : 537
    
```

Degenerated EF hand

```

      *           620           *           640           *
AtCRK1 : EKDGNRPTITHELASELGLGPSVVPVHVVLQDWIRHSDGKLSFLGFVRLH : 566
AtCRK2 : EMNGNRVIVITHELASELGVGSSIPVHTILNDWIRHSDGKLSFLGFVKLLH : 587
AtCRK3 : ETEGNRVITITHELARELNVCAS--AYGHLRDWVRS SDGKLSYLGFYKFLH : 583
AtCRK4 : EHEGNRITISVQELAGEMSVGPS--AYPLLRDWRSSDGKLSFLGYAKFLH : 582
AtCRK5 : EKEGNRPITIDELASELGLGPSVVPVHAVLHDWLRHSDGKLSFLGFVKLLH : 591
AtCRK6 : ESEGSRAISVQELAEEMSLGPN--AYPLLRDWRSSDGKLSFLGYAKFLH : 581
AtCRK7 : EKDGNRVITITHELASELGLGPSVVPVHVVLQDWIRHSDGKLSFLGFVRLH : 567
AtCRK8 : DKNGNRRAITITHELASELGVGPSIPVHSVLEHDWIRHSDGKLSFFGFVKLLH : 594
LeCRK1 : EQEGNRVISVEELAQEMNLGPT--AYAFLRDWRPSDRKLSFLGYTKFLH : 585
NtCBK1 : EQEGNRVISVEELAQEMNLGPT--AYAFLRDWRPSDRKLSFLGYTKFLH : 586
NtCBK2 : EKEGNRRAITITHELASELGLGPSVVPVHAVLHDWLRHSDGKLSFLGFVKLLH : 591
DcCRK1 : EKDGNRRAITITHELASELGLGPSIPVHAVLHDWIRHSDGKLSFLGFVKLLH : 591
ZmMCK1 : EQEGNRVISVEELAQEMNLGPT--HYSIVQDWIRKSDGKLSFLGFYKFLH : 613
ZmMCK2 : EQEGNRVISVEELAQEMNLGPT--HYSIVQDWIRKSDGKLSFLGFYKFLH : 595
OsCBK1 : DKEGNRPIVIDELASGLGLGPSVPLHVVLQDWIRHSDGKLSFLGFVKLLH : 587

```

Degenerated EF hand

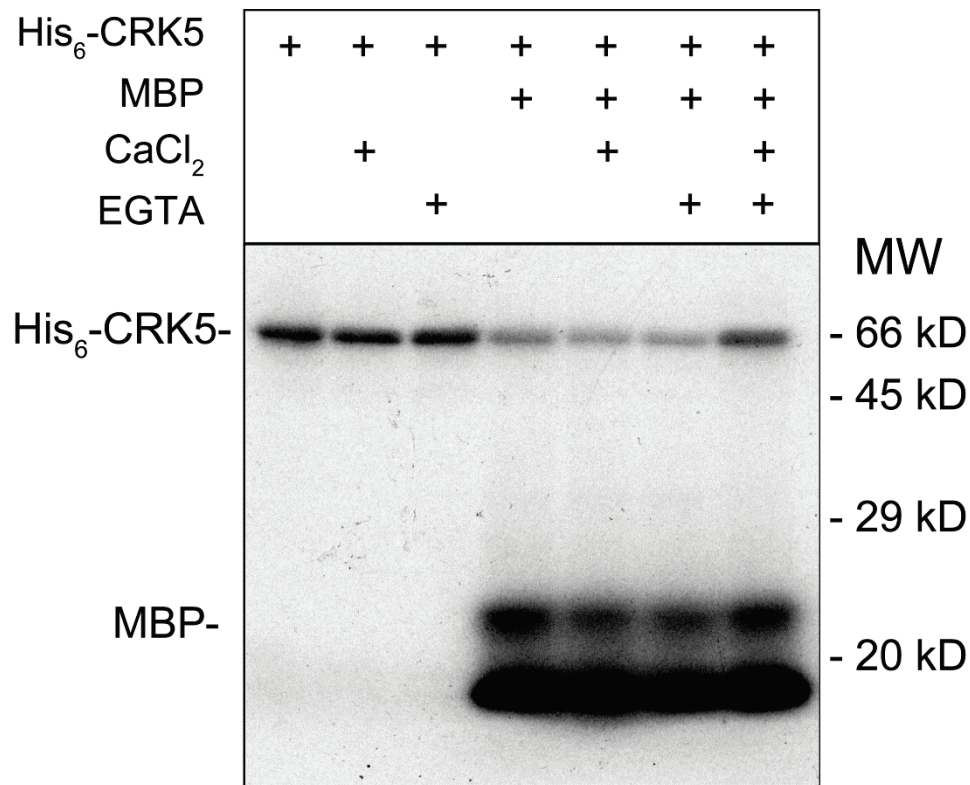
```

      660
AtCRK1 : GVSSR-TLQFA-- : 576
AtCRK2 : GVSTRQSLAATR- : 599
AtCRK3 : GVTLRAAHARPR- : 595
AtCRK4 : CVTVRSSSSRPR- : 594
AtCRK5 : GVSSR-TI-FAH- : 601
AtCRK6 : CVTVRSSSSRPMR : 594
AtCRK7 : GVSSR-TLQFA-- : 577
AtCRK8 : GVSVRASGKTTR- : 606
LeCRK1 : GVTMRSSSTRHHR : 598
NtCBK1 : GVTIRGSSTRHHR : 599
NtCBK2 : GVSSR-SITKIQ- : 602
DcCRK1 : GVSTR-AIAFAQ- : 602
ZmMCK1 : GVTIRGSNTRRH- : 625
ZmMCK2 : GVTIRGSNTRRH- : 607
OsCBK1 : GVSSR-TIPAT-- : 597

```

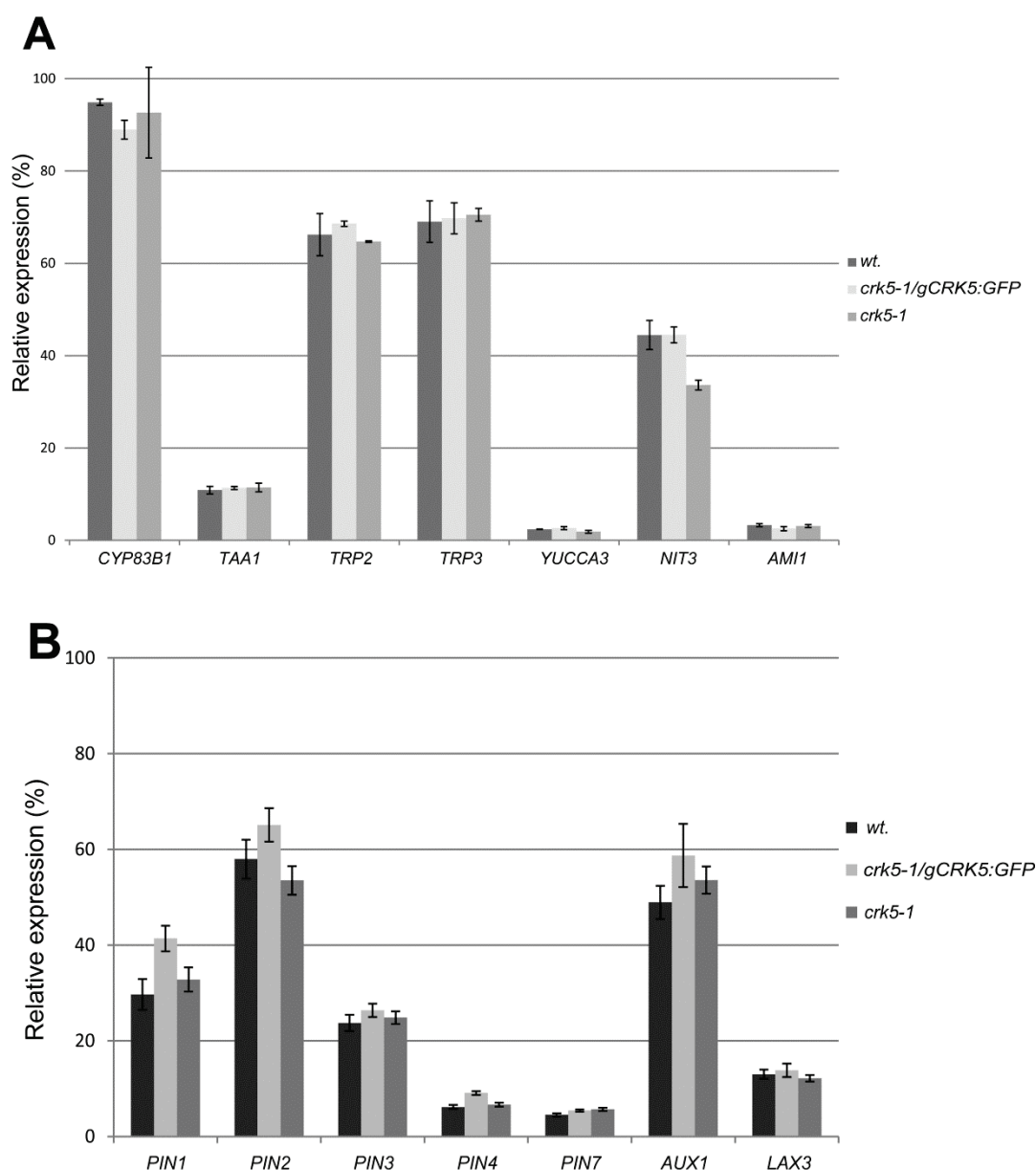
Supplemental Figure 3. Cobalt Sequence Alignment of Conserved Domains of CRK Family Members from Different Plant Species.

Members of the CRK family from different plant species carry highly conserved kinase catalytic domains but their N-terminal domains show a remarkable sequence divergence. Conserved myristolation, ATP-binding, T-loop, calmodulin-binding and degenerated EF hand motives of CRKs are indicated. GenBank (NCBI) accession numbers: CRK1 (At2g41140), CRK2 (At3g19100), CRK3 (At2g46700), CRK4 (At5g24430), CRK5 (At3g50530), CRK6 (At3g49370), CRK7 (At3g56760) CRK8 (At1g49580), LeCRK1 (AY079049), NtCBK1 (AF435450), NtCBK2 (AF435452), DcCRK1 (CAA58750), ZmMCK1 (AAB47181), ZmMCK2 (AF289237), OsCBK1 (AF368282). T-loop autophosphorylation sites identified in CRK3 and CRK6 (Hegeman et al., 2006) are indicated by blue shading.

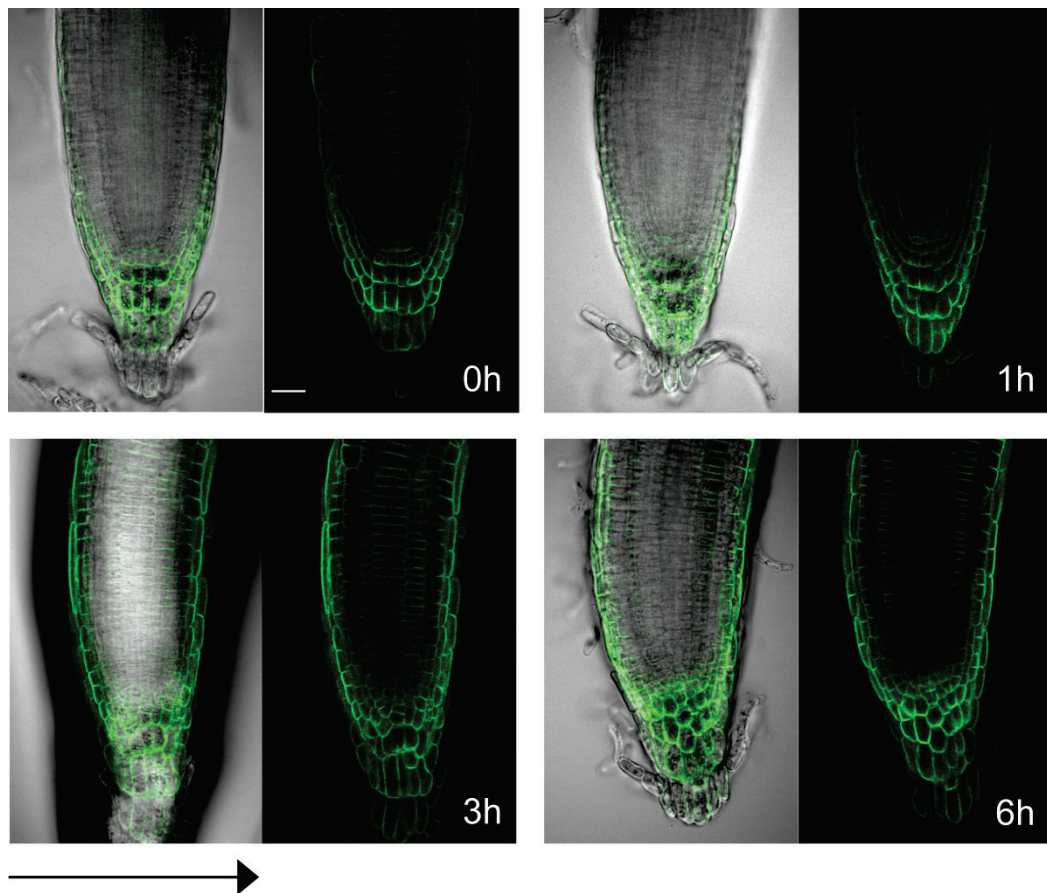


Supplemental Figure 4. *In vitro* Kinase Assays with Purified His₆-CRK5.

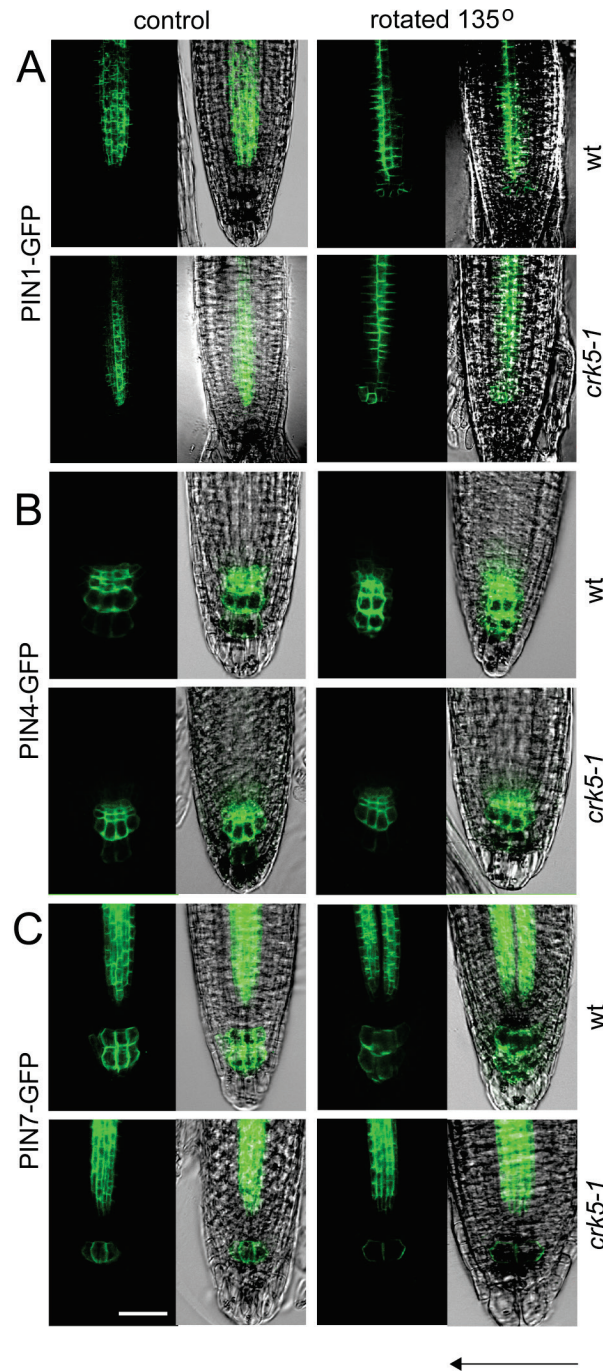
The phosphorylation assays were performed with 1 μg of His₆-CRK5 and 2 μg myelin basic protein (MBP) as artificial phosphorylation substrate at room temperature for 0.5h with or without addition of 0.1 mM Ca²⁺ and 1 mM EGTA alone or in combination as described in the Methods. The reaction products were separated by 12% SDS-PAGE. CRK5 autophosphorylation and CRK5-mediated MBP phosphorylation were detected subsequently by autoradiography.



Supplemental Figure 5. qRT-PCR Comparison of mRNA Levels of Genes Involved in the Regulation of Auxin Biosynthesis and Encoding PIN Auxin Efflux and AUX/LAX Influx Carriers in Roots of Wild Type, *crk5-1* Mutant and Genetically Complemented *crk5-1/gCRK5-GFP* Seedlings. (A) Comparison of transcript levels of *CYP83B1* (At4g31500), *TAA1* (At1g70560), *TRP2* (At5g54810), *TRP3* (At3g54640), *YUCCA3* (At1g04610), *NIT3* (At3g44320), and *AMI1* (At1g08980). (B) Relative transcript levels of *PIN1* (At1g73590), *PIN2* (At5g57090), *PIN3* (At3g70940), *PIN4* (At2g01420), *PIN7* (At1g23080), *AUX1* (At2g38120), and *LAX3* (At1g77690) normalized for *GAPDH2* (At1g13440). qRT-PCR measurements were performed in triplicates. Bars label standard error (SE) of measurements performed with three biological replicates.



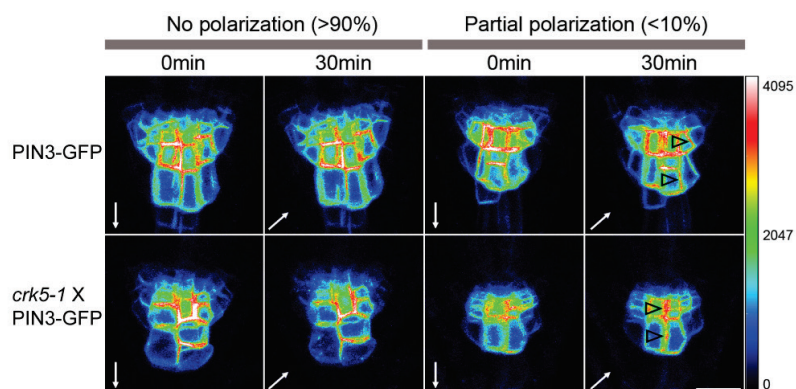
Supplemental Figure 6. Polar Localization of CRK5-GFP is not Changed in Root Cell Files in Response to Gravistimulation. Vertically grown 7-day-old seedlings were subjected to 135° rotation (0h) and CRK5-GFP localization was monitored at 1h, 3h and 6h after the start of gravistimulation. Bar 50 μ m.



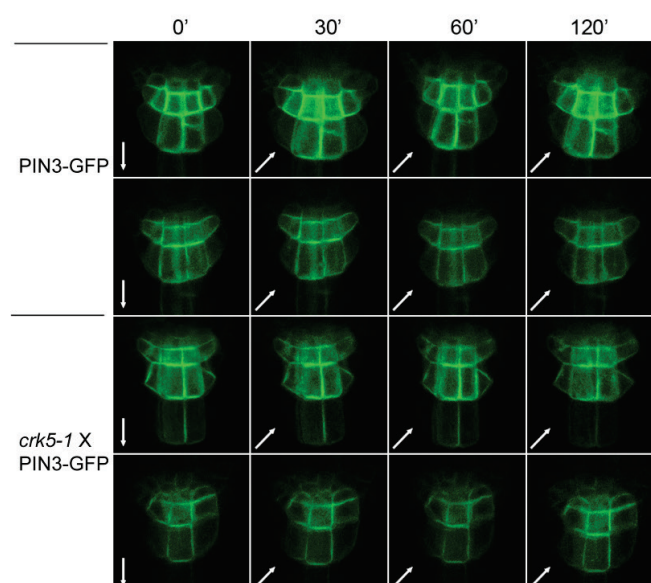
Supplemental Figure 7. Localization of PIN1-GFP, PIN4-GFP and PIN7-GFP in Vertically Grown and Gravistimulated Roots of Wild Type and *crk5-1* Mutant Plants.

(A to C) PIN1-GFP, (A) PIN4-GFP (B) and PIN7-GFP (C) expressing seedlings were grown for 7 days in vertical position, and then subjected to gravistimulation by 135° rotation for 20 h. Localization of PIN1-GFP is comparable between wild type and *crk5-1*. PIN4-GFP pattern is extended to the QC and adjacent layers of dividing cells during gravistimulation in wild type but not in the *crk5-1* mutant. Compared to wild type, the levels of PIN7-GFP is somewhat reduced in the vasculature of *crk5-1* roots.

A

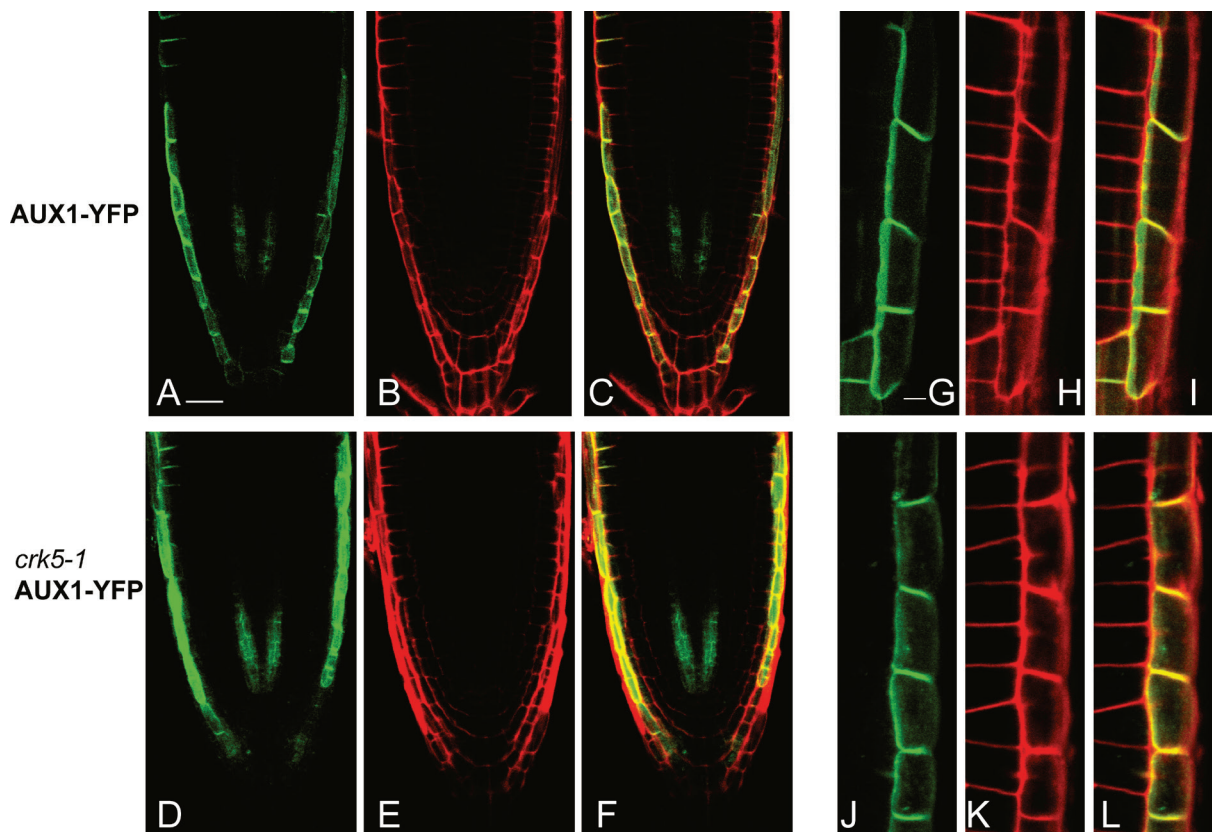


B



Supplementary Figure 8. Comparison of PIN3-GFP Localization in Vertically Grown and Gravistimulated Roots of Wild Type and *crk5-1* Mutant.

(A) Localization of PIN3-GFP in columella and root cap cells of wild type (wt) and *crk5-1* mutant. Color-coded heat map of Z-stack projections of 6 slices are shown before (0 min) and after 135° gravistimulation (30 min). Seedlings were categorized to "No Polarization" (apolar; >90%) and "Partial Polarization" (<10%) classes. Regions of partial polarization of PIN3-GFP are indicated by black triangles. White arrows indicate the gravity vector. Scale bar is 20 μm. (B) Time course analysis of PIN3-GFP localization in wild type (wt) and *crk5-1* mutant. Image at 0 min shows nonstimulated vertically grown root tips. Following gravistimulation of 4-day-old roots by 135° rotation, images were captured at 30, 60 and 120 minutes as mid optical sections of root columella cell layer. In both (A) and (B), at least 20 wild type and *crk5-1* seedlings were analyzed. Arrows indicate the gravity vector. Scale bar is 20 μm.



Supplementary Figure 9. Cellular Localization of AUX1-YFP in Wild Type and *crk5-1* Mutant Roots.

(A to F) Localization of AUX1-YFP in primary roots of 5-day-old wild type (A to C) and *crk5-1* (D to F) seedlings grown vertically in continuous light. (A, D) YFP signal, (B, E) counter-staining with propidium iodine, and (C, F) superimposed images of (A and B) and (D and E). (G to L) AUX1-YFP localization in the basal and internal lateral membranes of wild type (G to I) and *crk5-1* (J to K) lateral root cap cells. (G, J) YFP signal, (H, K) counter-staining with propidium iodine, and (I, L) superimposed images of (G and H) and (J and K).

Supplemental Table 1. List of PCR Oligonucleotide Primers.

Name	Sequence (5' to 3')	Gene number reference
CRK5BamHI-F	ctagggatccaaATGGGTCTATGTACTTCG	
CRK5XhoI-R	aggctactcgagCTAATGAGCTTTGATCG	
<i>crk5-1</i> F	CCGAATTCTCCTATTTTCTAGCTTCGGC	
<i>crk5-1</i> R	GGAGAATGAGACCTTAGAGCTCAGAC	
Fish1	CTGGGAATGGCGAAATCAAGGCATC	Ríos et al. (2002)
Fish2	CAGTCATAGCCGAATAGCCTCTCCA	Ríos et al. (2002)
<i>crk5-2</i> F	CACCGAATTCTCCTATTTTCTAGC	
<i>crk5-2</i> R	CCTCCTCTGTGTACTTCCCACC	
LBa1	TGGTTCACGTAGTGGGCCATCG	Alonso et. al. (2003)
1: CRK5-F1	AAGCGAACGTATCGTCGTTTC	
2: CRK5-R2	ATTGAGTACTTTGTCAATGGCGAAT	
3: CRK5-F3	GATTTTCGTGTGATGTTGAGAGATT	
4: CRK5-R4	GAAGTACATAGACCCATTTAAGAATCTCTC	
5: CRK5-F5	CAACGAACAATGAAGGCAAAA	
6: CRK5-R6	GATCTCGCCGGAGTCTTCTT	
8: CRK5-R8	TCATAACAAAAGTCAAAAGCCACA	
ACT2/8-F	GGTAACATTGTGCTCAGTGGTGG	At3g18780, An et al. (1996)
ACT2/8-R	AACGACCTTAATCTTCATGCTGC	At3g18780, An et al. (1996)
CRK5 Saul	TAAACTTACCTCAGGAAGTGGT	
CRK5 stop to ApaI	TTCAAAGTTTCAAAACCGGGCCCATGAGCTTTG ATCGTGC	
T3 primer	ATTAACCTCACTAAAGGGA	Stratagene
T7 primer	TAATACGACTCACTATAGGG	Stratagene
eGFP ApaI 5'	CATAAGGGCCCACCATGGTGAGCAAGGGCGAG GAGCTG	
eGFP ApaI 3'	AATATGGGCCCTTACTTGTACAGCTCGTCCATGC CGAG	
GUS ApaI 5'	CATAAGGGCCCACCATGTTACGTCCTGTAGAAA CCCCA	
GUS ApaI 3'	AATATGGGCCCTCATTGTTTGCCTCCCTGCTGCG GTTT	
CRK5-R1	GGGTCTATGTACTTCGAAACCGA	for real time PCR
CRK5-R2	TAACGGAAGAGCTCGAAGGC	for real time PCR
GAPDH-2-F	AATGGAAAATTGACCGGAATGT	At1g13440, Czechowski et al. (2005) for real time PCR
GAPDH-2-R	CGGTGAGATCAACAAGTGAAGACA	At1g13440, Czechowski et al. (2005) for real time PCR
PIN1-F	TGGAAGACAACCTTTGGAAACT	At1g73590
PIN1-R	TGAAGCATTAGAACGACGAACA	At1g73590
PIN2-F	CCTCGCCGCACTCTTTCTTT	At5g57090
PIN2-R	CGTACATCGCCCTAAGCAAT	At5g57090
PIN3-F	CAAGTGGAGATTTTCGGAGGA	At3g70940
PIN3-R	GCGTCTTTTGGTCTCTCTGC	At3g70940
PIN4-F	GGCAACGGAACAATCTGAAC	At2g01420
PIN4-R	TCACCACCACCTCTAGCATTAC	At2g01420
PIN7-F	AAGGCGGTGCAAAAGAGATT	At1g23080
PIN7-R	CATCGGACCAGCTTTGTTTT	At1g23080
AUX1-F	CTTTCCTCCTCTGCACATTTCT	At2g38120

AUX1-R	AAGAGTGGTTTTTGTCCGTTTG	At2g38120
LAX3-F	TGCTTACCTTTGCTCCTGCT	At1g77690
LAX3-R	GTCCCATCCATCCTCCTAC	At1g77690
CYP83B1-F	ACCCTAACCGCCCTAAACAAGA	At4g31500 Mei et al. 2011
CYP83B1-R	GTCAGTTCCCGGCACAACAATA	At4g31500 Mei et al. 2011
TAA1-F	TAAACACTATACAAACGACCAAACC	At1g70560 Mei et al. 2011
TAA1-R	TACACCTGTCACCCATCTTCCT	At1g70560 Mei et al. 2011
TRP2-F	TTGAATCCGCTTTCTATGCTCT	At5g54810 Mei et al. 2011
TRP2-R	CTGTAATGCTCCGTAAGCCTCT	At5g54810 Mei et al. 2011
TRP3-F	ATCATCTGTAAGCGGAAAGGTTC	At3g54640 Mei et al. 2011
TRP3-R	TTCAGTTGGCGACTTTGCATCAC	At3g54640 Mei et al. 2011
YUCCA3-F	CGTTCGTAGCGCTGTTTCATG	At1g04610 Mei et al. 2011
YUCCA3-R	CTAACGGTCCAATTTTCGGC	At1g04610 Mei et al. 2011
NIT3-F	AGGTTATTGGCGTTGACCCAT	At3g44320 Mei et al. 2011
NIT3-R	ATCTTCCACTTCAGGGCCAG	At3g44320 Mei et al. 2011
AMI-F	TCTACTTCCTCGTCGCCTCCT	At1g08980 Mei et al. 2011
AMI-R	GCGCATTTTCTCCGTTTATACTG	At1g08980 Mei et al. 2011

Supplemental Methods and References

Identification of *crk5* T-DNA Insertion Mutants

To screen for homozygous lines, segregation analysis of T2 families carrying T-DNA insertions in the *CRK5* gene was carried out as described (Ríos et al., 2002) using T-DNA and gene-specific primers (see Supplemental Table 1 online). By sequencing the PCR amplified left and right T-DNA border-plant DNA junctions, a single T-DNA insertion was localized 54 bp 3'-downstream of the ATG codon in exon 1. The T-DNA insertion generated a target site deletion of 10 bp. At the left border junction, facing the promoter, 21 bp was retained from the 25 bp border (capital letters) sequence (plant DNA-tcaaaactccggcg/AGGATATATTCAA TTGTAAAT-T-DNA), while the right border junction contained 1 bp from the border repeat (T-DNA-T/cacttccggcg-plant DNA). In the *crk5-2* allele, a single T-DNA insertion 167 bp 5'-upstream of the ATG generated a target site deletion of 24 bp. At the right T-DNA junction facing the promoter, a single nucleotide from the right border repeat was linked through a filler DNA (bold) sequence of 29 bp to *CRK5* sequences (plant DNA-aagtactcaat/AACACATTGCGGACGTTATTGTGGTGTAATA-T-DNA). At the left T-DNA junction 9 bp was retained from the 25 bp border repeat (T-DNA-GTTTACACC/acaacaatttt-plant DNA).

Plasmid Constructs and *Agrobacterium*-mediated Plant Transformation

A BpmI-BstXI fragment of 7809bp, carrying the full length *CRK5* gene with a promoter region of 4414 bp, was isolated from the BAC clone T20E23 obtained from the Arabidopsis Biological Resource Center. After treatment with DNA polymerase Klenow fragment, the *CRK5* gene was cloned into the SmaI site of vector pBluescript SK (pBSK), from which the ApaI site was previously removed, to obtain pBSKΔApaIgCRK5. Translational stop codon of *CRK5* was replaced by an ApaI site, and a SauI-SacII 3' segment of modified *CRK5* gene was amplified by a two-step PCR reaction using high fidelity Pfu DNA polymerase (Fermentas) and the pBSK T3, CRK5 SauI and CRK5 StoptoApaI primers (see Supplemental Table 1 online). Following digestion, the PCR amplified *CRK5* fragment was used for replacement of corresponding SauI-SacII segment of pBSKΔApaIgCRK5 to generate pBSKΔApaIgCRK5ApaI, carrying a single ApaI site replacing the *CRK5* stop codon. Coding regions of *GFP* and *uidA/GUS* were PCR amplified as ApaI fragments carrying 3' stop codons (see primers in Supplemental Table 1 online) and cloned into the single ApaI site of

pBSKΔApaI-gCRK5-ApaI to generate in frame 3'-translation gene fusions. The resulting gCRK5-GFP and gCRK5-GUS gene cassettes were isolated as PstI-NotI fragments and inserted into PstI-Ecl136II sites of the binary plant transformation vector pK7FWG2 (Karimi et al., 2002) by removing the Gateway cassette. Binary vectors were introduced into *Agrobacterium* GV3101 carrying either the pMP90 or pMP90RK Ti-helper plasmids as described (Koncz et al., 1994). Wild type and *crk5-1* mutant plants were transformed using the infiltration method (Bechtold et al., 1993). Primary (T1) transformants were selected on 0.5 MS medium containing either 30 μg/ml kanamycin or 15.75 mg/l sulfadiazine in case of DR5-GFP (Ottensschläger et al. 2003). Following segregation analysis of T2 families, T3 lines carrying single T-DNA insertions were identified. AUX1-YFP (Swarup et al., 2004), PIN1-GFP (Benková et al., 2003), PIN2-GFP (Xu and Scheres, 2005), PIN3-GFP (Zádníková et al., 2010), PIN4 -GFP and PIN7-GFP (Blilou et al., 2005) were introgressed by crosses into the *crk5-1* mutant followed by PCR-based genotyping of *crk5-1* homozygous lines and screening for lines carrying the AUX1 and PIN reporters in homozygous forms.

To express N-terminal fusion of CRK5 with a His₆-tag, the coding sequence of *CRK5* cDNA was PCR amplified and inserted by BamHI-XhoI into pET28c (Novagen). The coding sequence of the PIN2 hydrophilic T-loop (Müller et al., 1998) was PCR amplified and cloned as an EcoRI-BamHI fragment into pET28a. The pET28c-CRK5 and pET28aPIN2loop were transformed into the *E. coli* strain BL21(DE3) Rosetta (Novagen).

An YQ, McDowell JM, Huang S, McKinney EC, Chambliss S, Meagher RB (1996)

Strong, constitutive expression of the *Arabidopsis* ACT2/ACT8 actin subclass in vegetative tissues. *Plant J*, **10**: 107-121.

Bechtold, N., Ellis, J., and Pelletier, G. (1993). *In planta* *Agrobacterium* mediated gene transfer by infiltration of adult *Arabidopsis thaliana* plants. *C. R. Acad. Sci. Paris, Life Sciences*. **316**: 1194–1199.

Benková, E., Michniewicz, M., Sauer, M., Teichmann, T., Seifertová, D., Jürgens, G. and Friml, J. (2003) Local, efflux-dependent auxin gradients as a common module for plant organ formation. *Cell* **115**: 591-602.

Blilou, I., Xu, J., Wildwater, M., Willemsen, V., Paponov, I., Friml, J., Heidstra, R., Aida, M., Palme, K., and Scheres, B. (2005) The PIN auxin efflux facilitator network controls growth and patterning in *Arabidopsis* roots. *Nature* **433**: 39-44.

Czechowski T, Stitt M, Altmann T, Udvardi MK, Scheible WR (2005) Genome-wide identification and testing of superior reference genes for transcript normalization in *Arabidopsis*. *Plant Physiol*. **139**: 5-17.

Karimi, M., Inzé, D. and Depicker, A. (2002) GATEWAY vectors for *Agrobacterium*-mediated plant transformation. *Trends Plant Sci*. **7**: 193–195.

Koncz, C., Martini, N., Szabados, L., Hroudá, M., Bachmair, A., and Schell, J. (1994). Specialized vectors for gene tagging and expression studies. In: *Plant Molecular Biology*

- Manual, Gelvin, S., and Schilperoort, B. (eds.), Kluwer Academic Publishers, Dordrecht-Boston-London, **B2**: 1-22.
- Müller, A., Guan, C., Gälweiler, L., Tänzler, P., Huijser, P., Marchant, A., Parry, G., Bennett, M., Wisman, E., and Palme, K.** (1998) AtPIN2 defines a locus of Arabidopsis for root gravitropism control. *EMBO J.* **17**: 6903-6911.
- Ottenshläger, I., Wolff, P., Wolverton, C., Bhalerao, R.P., Sandberg, G., Ishikawa, H., Evans, M. and Palme, K.** (2003) Gravity-regulated differential auxin transport from columella to lateral root cap cells. *Proc. Natl. Acad. Sci. U.S.A.* **100**: 2987-2991.
- Swarup, R., Kramer, E.M., Perry, P., Knox, K., Leyser, H.M., Haseloff, J., Beemster, G.T., Bhalerao, R. and Bennett, M.J.** (2005) Root gravitropism requires lateral root cap and epidermal cells for transport and response to a mobile auxin signal. *Nat. Cell Biol.* **7**: 1057-1065.
- Zádníková, P., Petrášek, J., Marhavy, P., Raz, V., Vandenbussche, F., Ding, Z., Schwarzerová, K., Morita, M.T., Tasaka, M., Hejátko, J., Van Der Straeten, D., Friml, J. and Benková, E.** (2010) Role of PIN-mediated auxin efflux in apical hook development of *Arabidopsis thaliana*. *Development* **137**: 607-617.
- Xu, J. and Scheres, B.** (2005). Dissection of Arabidopsis ADP-RIBOSYLATION FACTOR 1 function in epidermal cell polarity. *Plant Cell* **17**: 525 -536.